

Editorial Manager(tm) for Journal of Fusion Energy
Manuscript Draft

Manuscript Number: JOFE-63

Title: Stellarator-mirror based fusion driven fission reactor

Article Type: Original Research

Keywords: fission-fusion hybrid; mirror; stellarator; RF heating

Corresponding Author: Dr. Vladimir E. Moiseenko, Ph.D.

Corresponding Author's Institution: NSC Kharkiv Institute of Physics and Technology

First Author: Vladimir E. Moiseenko, Ph.D.

Order of Authors: Vladimir E. Moiseenko, Ph.D.; K. Noack; Olov Ågren, Prof.

Stellarator-mirror based fusion driven fission reactor

V.E.Moiseenko^{1,2}, K.Noack³, O.Ågren¹¹ Uppsala University, SE-751 21Uppsala, Sweden² National Science Center "Kharkiv Institute of Physics and Technology"

61108 Kharkiv, Ukraine

³ Forschungszentrum Dresden-Rossendorf, 01328 Dresden, Germany

Keywords: controlled fusion, stellarator, mirror, sub-critical system, fast reactor.

Abstract

The version of fusion driven system (FDS), a sub-critical fast fission assembly with the fusion plasma neutron source, theoretically investigated here is based on a stellarator with a small mirror part. In the magnetic well of the mirror part, fusion reactions occur from collision of an RF heated hot ion component (tritium), with high perpendicular energy with cold background plasma ions. The hot ions are assumed to be trapped in the magnetic mirror part. The stellarator part which connects to the mirror part provides confinement for the bulk (deuterium) plasma. Calculations based on a power balance analysis indicate the possibility to achieve a net electric power output with a compact FDS device. For representative thermal power output of a power plant ($P_{th} \approx P_{fis} = 0.5-2GW$) the computed electric Q-factor is in the range $Q_{el} = 8-14$, which indicates high efficiency of the FDS scheme.

Corresponding author : V.E. Moiseenko

E-mail: moiseenk@ipp.kharkov.ua; Phone : +38 067 894 6013 ; Fax : +38 057 3352664.**I. Introduction**

In a sub-critical fast fission reactor the neutron multiplication factor k_{eff} , is less than unity. The coefficient k_{eff} is the average number of neutrons from a single fission that causes another fission. To sustain the fission reactions in a sub-critical system an external neutron source is therefore required to drive the fission power production. One option for the neutron source is an accelerator driven system (ADS) with a spallation neutron source. Another option is a fusion plasma neutron source, i.e. a fusion driven system (FDS). In sub-critical driven systems the fission rate is proportional to the external neutron flux intensity. In this way the fission chain is fully controlled that provides a superior safety for the sub-critical systems.

Several FDS studies have considered a tokamak based FDS [1]. An advantage of a tokamak is the achieved plasma confinement quality, but this scheme has also several disadvantages among which a few will be

1 remarked. The first is the high minimum power of a tokamak FDS. A small device would be beneficial for
2 scientific and technical research, but this is not possible with a tokamak FDS. A second drawback comes
3 from the fission mantle surrounding the plasma column, which restricts the access to the plasma. Some
4 discharge sustaining tokamak systems such as radio-frequency (RF) antennas have to operate inside the high
5 neutron flux reactor zone which causes technical problems. An FDS should preferably be able to run
6 continuously for years which is problematic for a tokamak which presently relies on pulsed inductive current
7 drive. These obstacles can be resolved by considering other plasma devices. For instance, in a recently
8 proposed FDS based on the Gas Dynamic Trap mirror device (which uses sloshing ions for neutron
9 generation) the fission mantle surrounds only a *part* of the plasma column where the sloshing ions are
10 trapped [2]. This gives a possibility to place neutral beam injection, plasma diagnostics etc. outside the
11 reactor active zone. However, for the reason of insufficient plasma energy confinement, the power efficiency
12 of such a scheme is low and it is positioned in [2] rather as a transmutation than an energy producing device.
13 The DRACON-based neutron source was proposed in [3]. It has a localized neutron output at the mirror
14 parts. The DRACON, a hybrid stellarator-mirror consists of two long open trap parts connected together by
15 two special stellarator (CREL) elements. A particular design of the CRELs would prevent penetration of the
16 Pfirsch-Schlüter currents into the open traps and provides a possibility to sustain a mirror confined high-beta
17 plasma there. If the two mirror parts are short, the penetration of the stellarator equilibrium currents to the
18 mirrors does not dramatically decrease the stellarator beta. In this case, instead of DRACON, which is still
19 not studied sufficiently neither theoretically nor experimentally, a stellarator with a small mirror part could
20 have almost the same efficiency. The assumption that a proper stellarator-mirror magnetic field could be
21 created can be supported by experience from other stellarator devices. Mirror parts were present in earlier
22 stellarators of the "racetrack" type, namely Model-C [4] and Uragan [5]. These devices had two straight parts
23 without rotational transform, and there was also an option to lower the magnetic field at the straight parts for
24 magnetic beach heating at the ion cyclotron frequency. The Wendelstein branch of stellarators is also often
25 presented as a linked mirror concept [6].

51 **II. Fusion-fission reactor scheme and computation model**

52 To generate neutrons, at least one ion component have to be hot enough. Hot ions are badly confined in a
53 stellarator. Some of them leave the stellarator rapidly owing to the gradient drift in the confining magnetic
54
55
56
57
58
59
60
61
62
63
64
65

1 field. The rate of such loss of ions is proportional to their energy. Thus, hot ions escape from the stellarator
 2 much faster than the background plasma ions.
 3

4 The FDS version under study here (see Fig.1) consists of a stellarator with a small mirror part with lower
 5 magnetic field containing a two-ion component plasma. The goal of the mirror part in this proposed hybrid
 6 magnetic trap is to improve the hot ion confinement. If the mirror is non-axisymmetric and has a minimum B
 7 property, MHD stabilization is provided and considerable values of hot ion beta values are achievable.
 8 Despite that the stellarator part does not confine efficiently hot ions, it confines well the background plasma,
 9 allowing for a higher electron temperature than can be provided by the open trap part solely. The hot ions can
 10 be sustained by neutral beam injection to the open trap part [2]. Another option is usage of ion cyclotron
 11 heating, which can be arranged by antennas located at the stellarator part far from the mirror region with the
 12 high neutron flux. The antenna field couples to the plasma, the waves propagate along the plasma column,
 13 reach the mirror part, propagate further to lower values of the magnetic field and becomes absorbed near the
 14 cyclotron resonances in the mirror part. The regime of RF heating could be chosen so, that the ion cyclotron
 15 resonance condition is met only at the mirror part. To trap the hot ions at the mirror part, the perpendicular
 16 ion temperature ought be higher than the parallel. This is provided by the ion cyclotron heating which
 17 increases mainly the perpendicular ion energy. Fusion neutrons are generated at the location of the hot ions,
 18 at the mirror part. It is surrounded by a mantle of fission materials in which the fusion neutrons initiate
 19 fission of the nuclear fuel with a successive neutron multiplication.
 20

21 The hot ion energy balance is influenced by the electron drag. It dominates over the ion-ion collisions since
 22 the ratio of perpendicular hot ion temperature to the background plasma temperature is high, i.e.
 23 $T_{\perp} / T_{bg} > 50$. The ion-cyclotron heating increases the hot ion perpendicular energy. The parallel hot ion
 24 temperature T_{\parallel} appears in a balance of two factors: pitch angle scattering of the hot ions by the background
 25 ions which increases T_{\parallel} and the electron drag that tends to decrease it. The parallel energy balance can be
 26 written
 27

$$28 \frac{1}{2} \frac{d(n_{hi} T)}{dt} = (\nu_{ii}^{\perp} - \nu_{ie}^{\parallel}) n_{hi} T_{\parallel} / 2 = 0, \quad (1)$$

29 where n_{hi} is the hot ion density in the mirror part, ν denotes collision frequencies and v_T stands for thermal
 30 velocities, and
 31

$$32 \nu_{ii}^{\perp} = \frac{2\pi^{1/2} Q_{00}}{m_i^2 v_{Ti\perp} v_{Ti\parallel}^2}, \quad (2)$$

$$v_{ie}^{\parallel} = -\frac{8Q_{00}}{3\pi^{1/2}m_e m_i v_{Te}^3}, \quad (3)$$

$Q_{00} = 4\pi e_i^2 \omega_p^2 n_{bg}$, e denotes ion charge and n_{bg} is the background plasma density.

The expression for the hot ion distribution anisotropy factor

$$F = T_{\perp} / T_{\parallel} = \frac{4}{3\pi} \sqrt{m_e / m_i} (T_{\perp} / T_{bg})^{3/2} \quad (4)$$

is obtained from equations (1-3). Formula (4) shows that a reasonable anisotropy factor requires a high value of the ratio of hot ion energy to the background temperature and depends on it sensitively. To sustain the same ion distribution anisotropy the ion energy should vary proportionally to the background plasma temperature. If the background plasma temperature is high it is difficult to sustain a strongly anisotropic hot ion distribution and, in the same time, to provide high neutron generation rate.

The beta values at the stellarator and open trap parts are limited by the maximum values β_{st} and β_{mir} , where

$$\beta_{st} = \frac{16\pi k_B n_e T_e}{B_0^2}, \quad \beta_{mir} \approx \frac{8\pi k_B n_i T_{\perp}}{B_{mir}^2}. \quad (5)$$

Here $k_B = 1,602 \cdot 10^{-12} \text{ erg} / eV$. Knowing these constants, the particle densities at the mirror parts can be calculated

$$n_{bg} = \frac{\beta_{st} B_0^2}{32\pi k_B T_{bg}}, \quad n_{hi} = \frac{\beta_{mir} B_0^2}{8\pi k_B T_{\perp} R^2}. \quad (6)$$

To use formula (6) one needs to determine the mirror ratio $R = B_{st} / B_{mir}$. It could be chosen from the

requirement that the condition of the particle confinement in the mirror

$$v_{\parallel}^2 / v_{\perp}^2 < R - 1. \quad (7)$$

should be satisfied by the majority of the hot ion velocity distribution. This means that the confinement factor

$$G = (R - 1) T_{\perp} / T_{\parallel} > 1. \quad (8)$$

should not be small. There is no need to make G too large because the distribution function decreases

exponentially in the velocity space aside the bulk region. The mirror ratio which satisfies the requirement (8)

is typically small.

If this is fulfilled, the hot ions are confined well in the mirror part and the major channel for the energy loss is

the electron drag. The RF heating power compensates the power of the electron drag in the mirror part

$$P_{RF} \approx P_d = v_{ie} k_B n_i T_{\perp} V R \eta, \quad (9)$$

where $V = 2\pi^2 a^3 \varepsilon$, $\varepsilon = a/R_{tor}$ is the reverse aspect ratio of the torus, a is the minor radius, R_{tor} is the torus major radius, $\eta = L/(2\pi R_{tor})$ and L is the length of the mirror part of the device. The electron drag which is characterized by the rate coefficient

$$\langle \sigma_{ie} v \rangle = C_{\sigma} / T_e^{3/2} \quad (10)$$

dominates in the hot ion energy losses, where $C_{\sigma} = \frac{4\sqrt{2\pi}}{3} \frac{e^4 \lambda_{col} \sqrt{m_e}}{m_i k_B^{3/2}} = 1.19 \cdot 10^{-8} \text{ cm}^3 \text{ eV}^{3/2} / \text{ s}$,

for tritium. The power leakage from the stellarator owing to the transport losses is

$$P_{tr} = 3k_B n_{bg} T_{bg} V / \tau_E \quad (12)$$

The energy confinement time τ_E is determined by the *ISS04* scaling [7]

$$\tau_E = C_E a^{2.28} R_{tor}^{0.64} P^{-0.61} n_{bg}^{0.54} B_0^{0.84} I^{0.41} \quad (13)$$

In CGS units $C_E = 3.69 \cdot 10^{-14}$. Equating the electron drag power (9) and the transport power (12), the plasma minor radius can be calculated

$$a^{1.09} = 3 \frac{2^{1.5} \pi^{1.54} k_B^{0.93} \beta_{st}^{0.07} \varepsilon^{0.03} T_{bg}^{1.52}}{C_{ie}^{0.39} C_E (\eta/R)^{0.39} \beta_{mir}^{0.39} B_0^{1.48} I^{0.41}} \quad (14)$$

The size of the machine increases with the background plasma temperature and decreases with the confining magnetic field. It does not depend explicitly on T_{\perp} . This dependence is represented by the dependence on β_{mir} . The torus minor radius is almost insensitive to the variation of β_{st} and the reverse aspect ratio ε . It is nearly inversely proportional to C_E . For a hybrid stellarator-mirror machine the energy confinement time could be smaller than for a regular stellarator. This corresponds to smaller C_E . But, following (14), the decrease in C_E could be compensated by increase of the confining magnetic field.

The hot ion perpendicular temperature T_{\perp} should be high enough to provide efficient D-T fusion and neutron generation. The efficiency of neutron generation is characterized by the target function

$H = \langle \sigma_{DT} v \rangle / T_{\perp} \propto p_{DT} / p_{RF}$ which is proportional to the ratio of fusion to RF heating power densities. The

function H is plotted in Fig.2. It has a maximum at $T_{\perp \max} = 83 \text{ keV}$, and its half-value tolerance range

$$30 \text{ keV} < T_{\perp} < 277 \text{ keV} \quad (15)$$

is very broad. The hot ion temperature is expected to be within the region given by Eq. (15).

III. Calculation parameters and results

The majority of the calculations are performed for hot tritium ions and a deuterium background plasma. To keep the hot ion velocity distribution anisotropy $F = T_{\perp} / T_{\parallel} = 5.7$ constant through the calculations, a constant value $T_{\perp} / T_{bg} = 100$ has been taken for the ratio of the tritium perpendicular temperature to the background plasma temperature. For higher tritium anisotropy it is hard to provide equilibrium and stability. We choose $\beta_{st} = 0.01$ and $\beta_{mir} = 0.15$, i.e. $\beta_{mir} < 1/F$. The mirror ratio is $R = 1.5$ which provides mirror confinement of the hot ions with a factor $G = 2.85$. The hot ion concentration at the mirror part $C_T = n_{hi} / n_{bg}$ is independent of the perpendicular temperature and equals $C_T = 0.13$. We vary the background plasma temperature, and correspondingly the hot ion temperature in the range (15), and calculate the plasma density, the heating power, the fusion power P_{fus} and the device dimensions. The fission power $P_{fis} = C_m P_{fus}$ is proportional to the fusion power. Since in our scheme the fission reactor part is similar to the one calculated in [2] the power multiplication coefficient is estimated using the results of that paper, and is chosen as $C_m = 120$ that is lower than in regular cases. The electric Q-factor is estimated as $Q_{el} = C_{RF} C_{ec} P_{fis} / P_{RF}$, where the RF heating efficiency is assumed to be $C_{RF} = 0.625$ and the thermal power conversion efficiency is $C_{ec} = 0.4$. In the calculations the inverse aspect ratio is $\varepsilon = 0.05$ and the normalized length of the mirror part is taken $\eta = 0.1$.

Figs. 3 and 4 show the plasma density and the torus minor and major radius and open trap length variations with the background ion temperature for different values of the confining magnetic field. With a constant β_{st} in Eq. (5), the plasma density is inversely proportional to the background temperature. The dependence on machine sizes comes from (14). At high background plasma temperature and low magnetic field the calculated sizes are huge, while at low temperature and high magnetic field they are too small. Thus the magnetic field should be chosen to fit the size of neutron generating part of the device with the fission mantle, i.e. the magnetic field would be small for a small-scale device and high for power plant scale machine.

The calculations for neutron emission intensity, total thermal power and the electric Q (see Figs. 5-6) involve the neutron emission calculations. These figures are almost independent on the confining magnetic field value although the magnetic field strength influences on the machine dimensions. For the case related to a power plant, total thermal power is $P_{th} = P_{fus} = 2.5 \text{ GW}$ which corresponds to the electric output $P_{el} = 1 \text{ GW}$

1 at $T_{bg} = 1.6keV$. The value $Q_{el} = 15$ of the electric Q is high enough at this point. The plot for Q_{el} shows a
2
3 rapid rise with the background temperature and is higher than unity starting from $T_{bg} = 340eV$. The rise in
4
5 Q_{el} with the background temperature saturates after the perpendicular ion temperature passes through its
6
7 optimum value. At the electric Q plot, the curve corresponding to hot deuterium and warm tritium is shown.
8
9 To equate the velocity anisotropy factor F , the ratio of perpendicular to the hot ion temperature in this case
10
11 is decreased by the factor $(m_T/m_D)^{1/3}$. The electric Q for hot deuterium is almost the same as for hot tritium
12
13 at low background temperatures and somewhat lower at high temperatures. For $T_{bg} = 1.6keV$, $Q_{el} = 12$ and
14
15 thermal power is $P_{th} = 2GW$ for the case of hot deuterium.
16
17
18

19 **Conclusions**

20
21 The combination of a stellarator and mirror is beneficial to localize the fusion neutron flux to the mirror part
22
23 of the device which is surrounded by a fission mantle. Two scenarios could be realized in the machine: hot
24
25 tritium in warm deuterium plasma and vice versa. Both scenarios are efficient with some advantage of the
26
27 first. The design and operation of all plasma device systems is facilitated with a localization of the neutron
28
29 emission. The calculations indicate promising potentials for the studied FDS scheme. In a wide range of the
30
31 machine parameters, a high electric Q is calculated. In a power plant scale the plasma part of the considered
32
33 FDS machine is rather compact with a size comparable to existing fusion devices. An experimental device
34
35 could be built in small scale for a proof-of-principle purpose, and even under these conditions it may have a
36
37 positive power output. Besides the commercial potential, a practical usage of such FDS would contribute to
38
39 the knowledge of fusion plasma handling.
40

41 **Acknowledgement**

42 This work is supported in part by a grant from Swedish Institute.
43
44

45 **References**

- 46
47 [1] Wu Bin, Fusion Engineering and design, 66-68, 181-186 (2003).
48
49 [2] K. Noack, A. Rogov, A. A. Ivanov, E. P. Kruglyakov, Fusion Science and Technology 51, · No.
50
51 2T, 65 (2007).
52
53 [3] V.E. Moiseenko, Transactions of Fusion Technology 27, 547 (1995).
54
55 [4] M.A. Rothman, R.M. Sinclair, I.G. Brown and J.C. Hosea, Phys. Fluids 12, 2211 (1969).
56
57 [5] V.F. Aleksin, O.V. Biryukov, A.V. Georgievskii et al, Atomic Energy 28, 25 (1970).
58
59 [6] F. Wagner, S. Bäuml, J. Baldzuhn et al, Phys. Plasmas 12, 072509 (2005).
60
61
62
63
64
65

[7] H. Yamada, J.H. Harris, A. Dinklage et al, Nucl. Fusion 45, 1684 (2005).

Figure captions

Fig.1. Sketch of fusion driven fission reactor.

Fig.2. The dependence of target function H on the hot ion perpendicular energy.

Fig.3. Plasma density as a function of background plasma temperature for different values of the magnetic field (triangle marker - $B_0 = 2T$, circle marker - $B_0 = 3T$,square marker - $B_0 = 4T$, cross marker - $B_0 = 5T$).

Fig. 4. Tore minor and major radii and mirror length as functions of background plasma temperature for different values of the magnetic field.

Fig. 5. Neutron emission intensity and output thermal power as functions of background plasma temperature.

Fig. 6. Electric Q as a function of background plasma temperature for hot tritium in warm deuterium plasma and hot deuterium in warm tritium plasma.

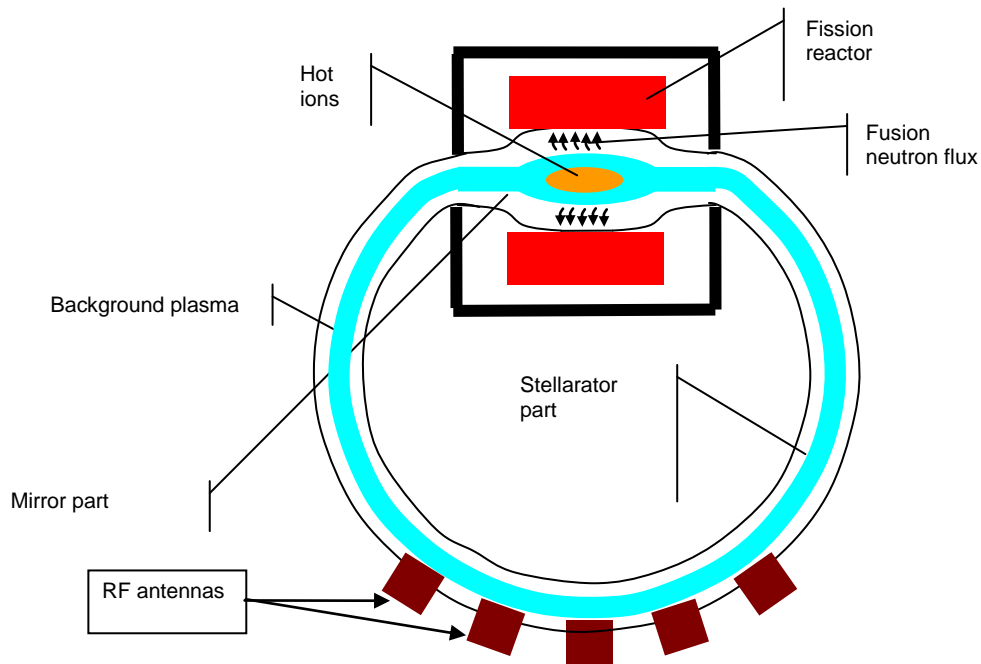


Fig.1.

1
2
3
4
5
6
7
8
9
10
11
12
13
14
15
16
17
18
19
20
21
22
23
24
25
26
27
28
29
30
31
32
33
34
35
36
37
38
39
40
41
42
43
44
45
46
47
48
49
50
51
52
53
54
55
56
57
58
59
60
61
62
63
64
65

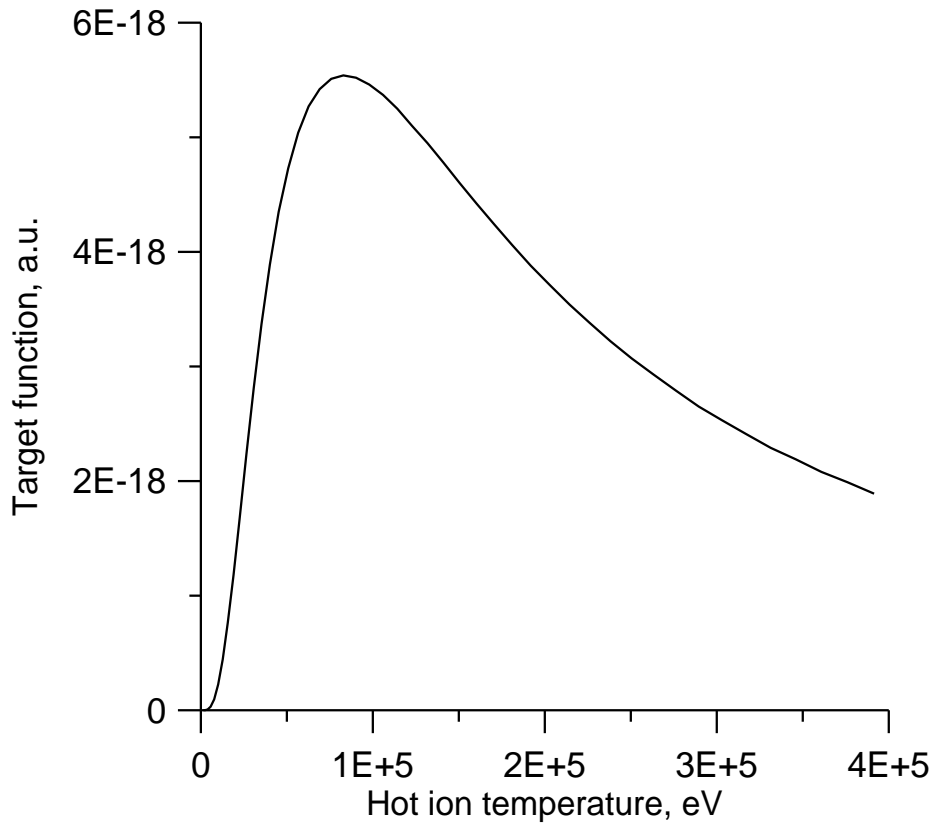


Fig.2

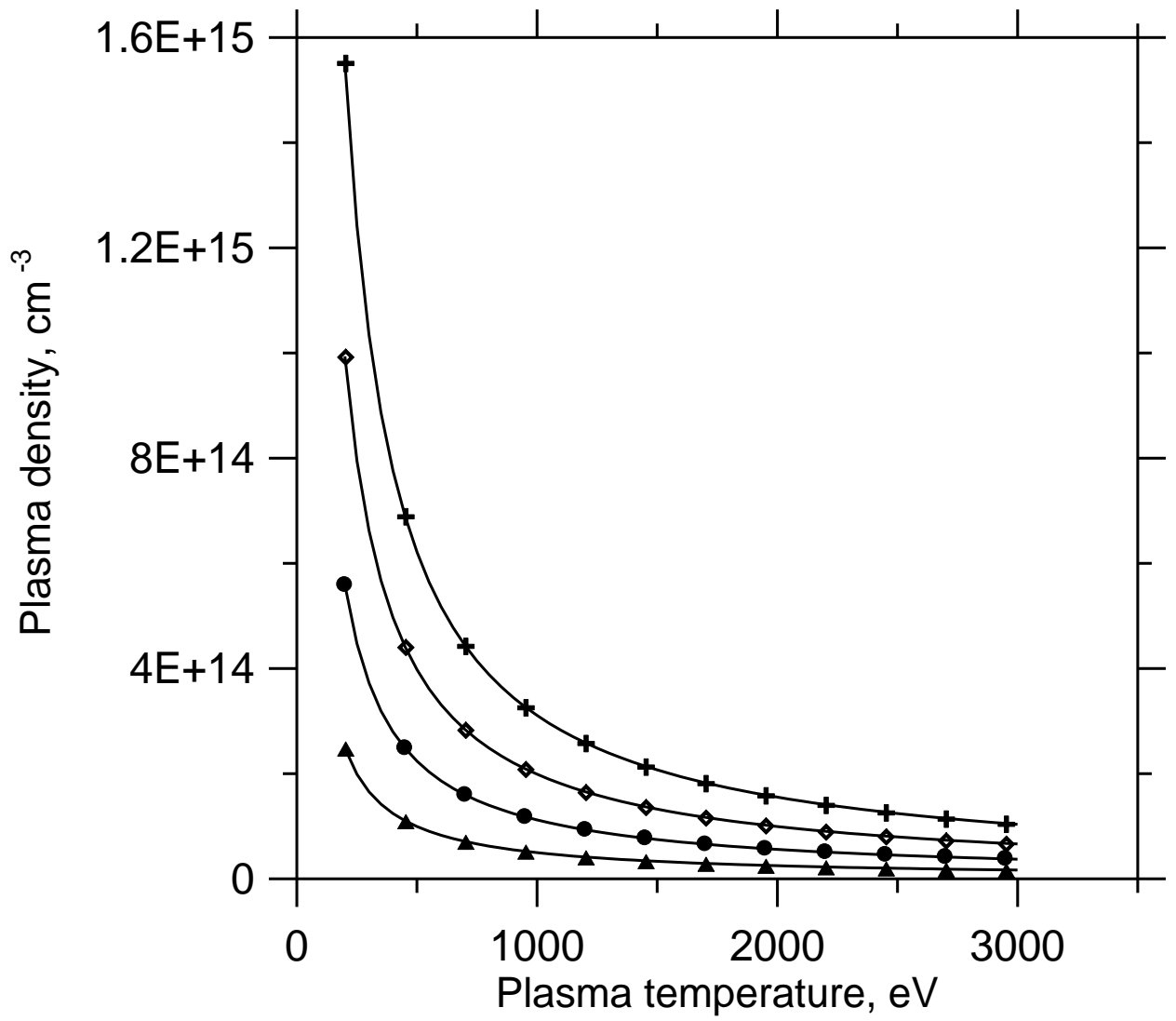


Fig. 3.

1
2
3
4
5
6
7
8
9
10
11
12
13
14
15
16
17
18
19
20
21
22
23
24
25
26
27
28
29
30
31
32
33
34
35
36
37
38
39
40
41
42
43
44
45
46
47
48
49
50
51
52
53
54
55
56
57
58
59
60
61
62
63
64
65

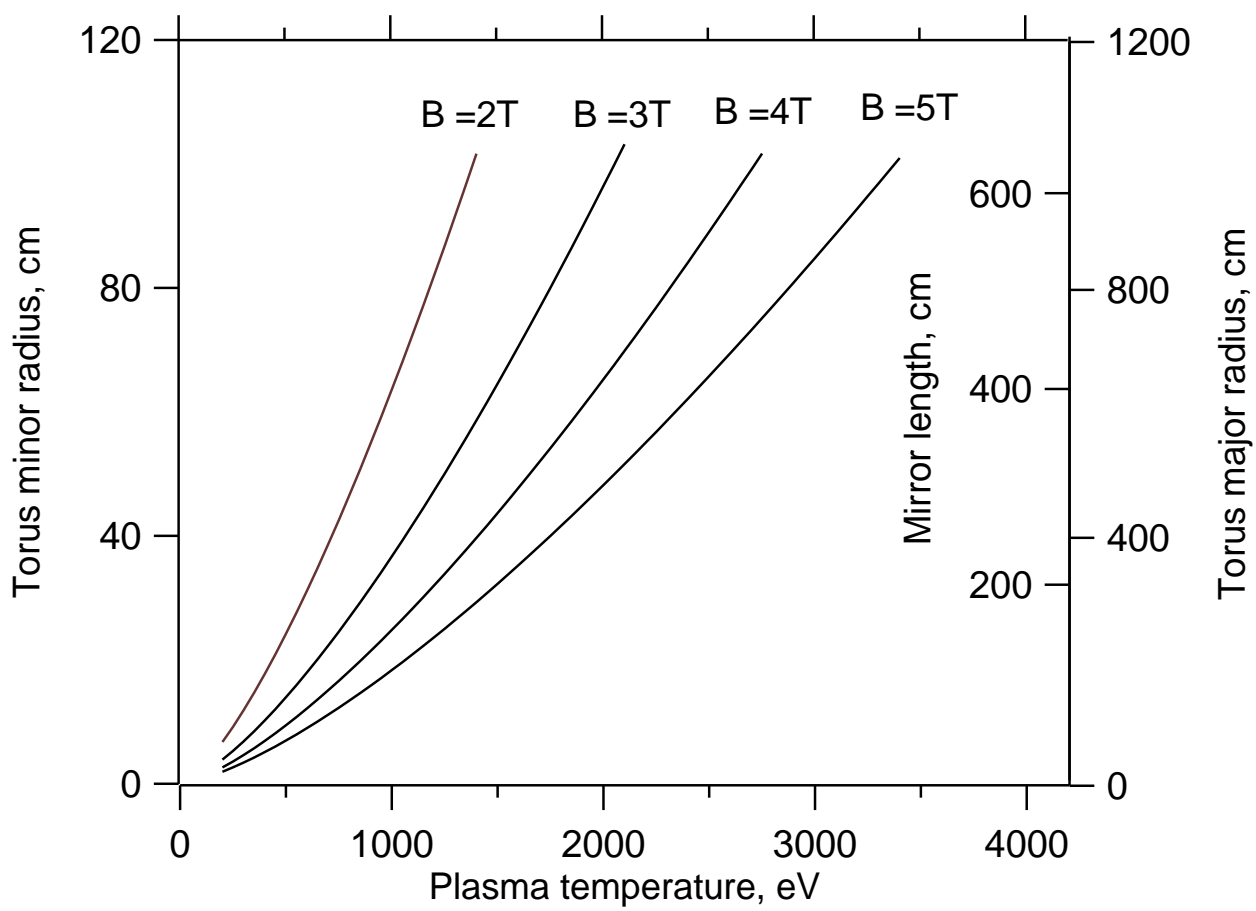


Fig.4.

1
2
3
4
5
6
7
8
9
10
11
12
13
14
15
16
17
18
19
20
21
22
23
24
25
26
27
28
29
30
31
32
33
34
35
36
37
38
39
40
41
42
43
44
45
46
47
48
49
50
51
52
53
54
55
56
57
58
59
60
61
62
63
64
65

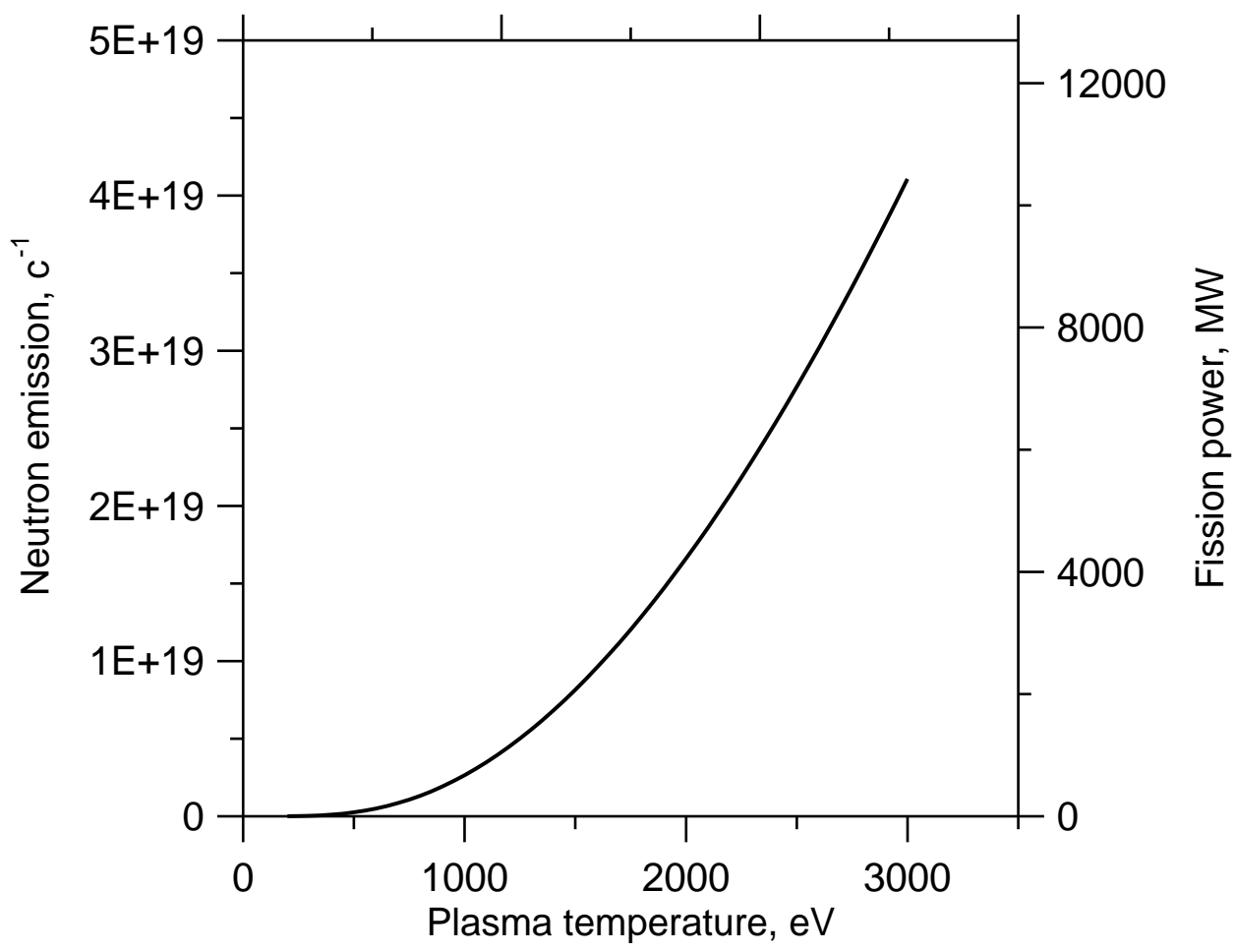


Fig.5.

1
2
3
4
5
6
7
8
9
10
11
12
13
14
15
16
17
18
19
20
21
22
23
24
25
26
27
28
29
30
31
32
33
34
35
36
37
38
39
40
41
42
43
44
45
46
47
48
49
50
51
52
53
54
55
56
57
58
59
60
61
62
63
64
65

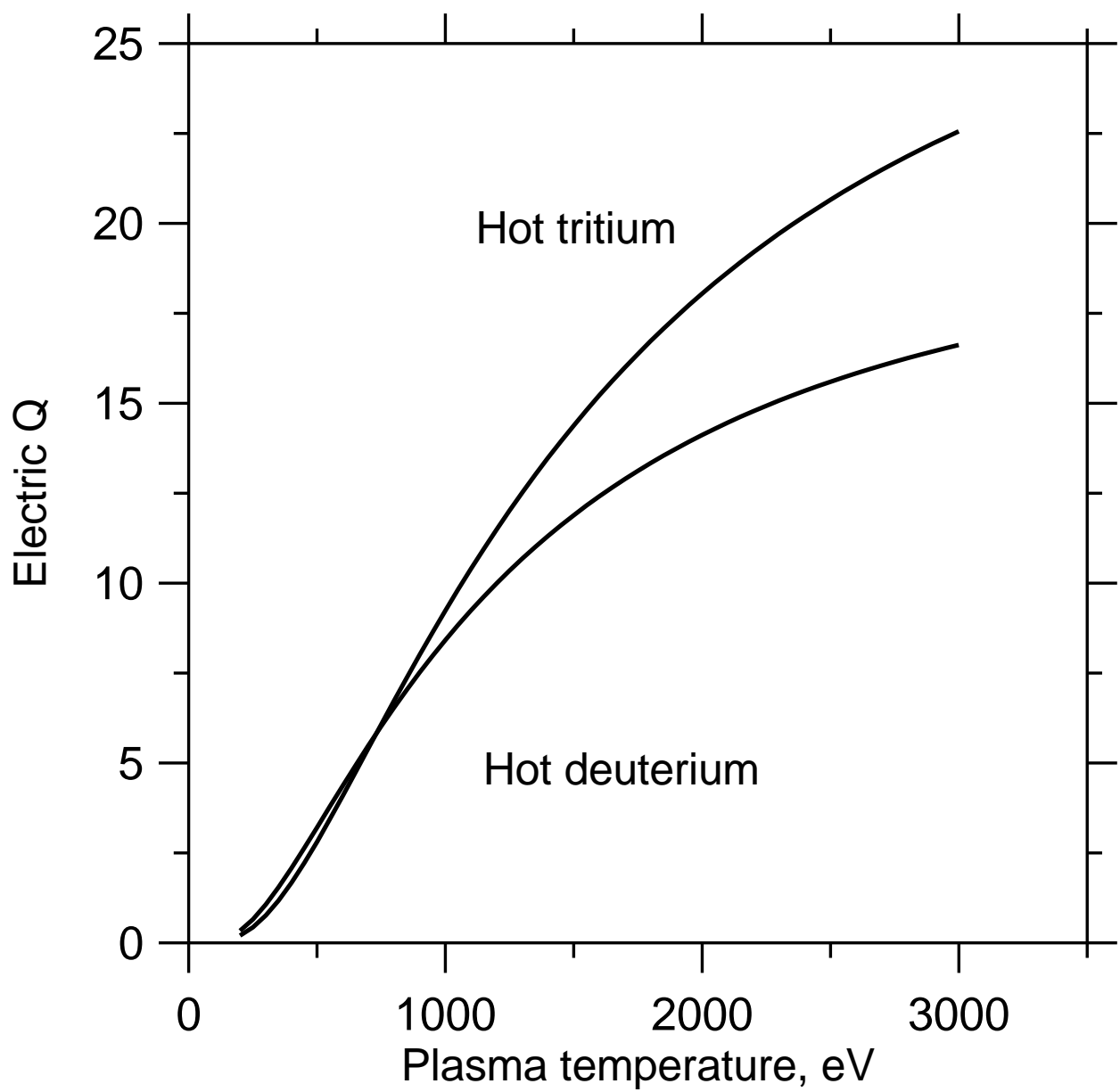


Fig. 6.